

Nucleocapsid Mass and Capsomer Protein Stoichiometry in Equine Herpesvirus 1: Scanning Transmission Electron Microscopic Study

WILLIAM W. NEWCOMB,¹ JAY C. BROWN,^{1*} FRANK P. BOOY,² AND ALASDAIR C. STEVEN²

Department of Microbiology and Cancer Center, University of Virginia Health Sciences Center, Charlottesville, Virginia 22908,¹ and Laboratory of Physical Biology, National Institute of Arthritis, Musculoskeletal and Skin Diseases, Bethesda, Maryland 20892²

Received 23 January 1989/Accepted 17 May 1989

The Brookhaven scanning transmission electron microscope was employed to measure the masses of two nucleocapsid species (of light and intermediate densities) of equine herpesvirus 1. These were found to be 196.7 ± 9.2 and 229.0 ± 9.5 megadaltons (MDa), respectively. Biochemical assays showed that neither nucleocapsid contained any significant amount of DNA ($<0.2\%$ [wt/wt]). Taking into account data on protein composition, we conclude that the difference between their masses is essentially contributed by viral protein 22 (46 kDa), which is an integral component of the maturable intermediate nucleocapsid but not of the abortive light nucleocapsid. In view of earlier ultrastructural information on capsomer symmetry, our mass determinations are consistent only with the 150 hexavalent capsomers being hexamers of the 148-kDa major capsid protein.

Herpesviruses have morphologically characteristic nucleocapsids whose surface shells (capsids), ~110 nm in diameter, contain the internal proteins and (eventually) the viral DNA (3, 7). The capsid is icosahedral of triangulation class $T = 16$ and is thus composed of 162 capsomers (38). Of these, 12 are pentavalent (i.e., having five nearest neighbors) and are located at the vertices of the icosahedron, while 150 are hexavalent and reside on its facets. Electron microscopy has shown that the hexavalent capsomers are roughly cylindrical, with a diameter of ~10 nm, a height of ~14 nm, and an axial channel that extends inwards at least part of the way from the outer surface (7, 38).

Nucleocapsids of several herpesviruses have been purified, and biochemical analyses have shown them to contain four to seven distinct proteins plus various amounts of DNA (3, 5). In the equine herpesvirus 1 (EHV-1) system, three distinct species of nucleocapsids have been separated on density gradients (19, 20) and correlated with the *in vivo* assembly pathway by means of pulse-chase experiments (21). Of the two lower-density species, light nucleocapsids were found to be abortive, whereas intermediate nucleocapsids, which complementary analyses suggested contained one or two additional minor proteins not found in light nucleocapsids, were concluded to be maturable. An attractive hypothesis emerging from these experiments (and supported by recent studies [23, 24, 27] with herpes simplex virus type 1) was that the additional proteins play a functionally vital role in distinguishing a maturable precursor particle from an abortive by-product of the assembly pathway. However, a general problem in such situations is how to be sure that minor components detected in biochemical assays are indeed integral constituents of designated particles and not comigrating contaminants.

All herpesvirus nucleocapsids contain one major protein, called protein 9 (p9) in EHV-1 and protein 5 (p5) in herpes simplex virus types 1 and 2, which has a molecular weight of 148 to 155 kilodaltons (kDa) (in different herpesvirus species) and which accounts for 55 to 75% of the total protein. It is widely accepted that this protein is the major constituent of (at least) the hexavalent capsomers (34). Its oligomeric

status, however, is less clearly defined. Sixfold symmetry has been inferred from negatively stained projection images (1, 18), most recently and quantitatively in terms of rotational power spectra (4, 29), suggesting that the capsomer is a hexamer. This stoichiometry is also consistent with calculations based on measurements of the DNA-to-protein ratio of herpes simplex virus type 1 virions (8). On the other hand, the alternative possibility of a trimer (33) is not ruled out, in the sense that a trimer of bilobed subunits could, at moderate resolution (~2.5 nm [29]), have a sixfold appearance. A suggestive precedent is given by the corresponding protein of adenovirus, also a large double-stranded DNA-containing virus with an icosahedral capsid of a high-order, nonskew triangulation class (22). The adenovirus hexon is now known from high-resolution crystallographic studies to be a trimer, but it has a pseudosixfold base (25). Under certain negative staining conditions, it presents a sixfold appearance (15).

We have addressed the two issues outlined above by using scanning transmission electronic microscopy (STEM) of unstained specimens (33, 35) to measure the respective masses of purified light and intermediate EHV-1 nucleocapsids. Since these measurements relate directly to individual, morphologically defined particles, they provide a basis for comparison that is not compromised by the possible presence of contaminants, i.e., molecules that are present in the same gradient fractions but are not bound to nucleocapsids. The data also serve to resolve the question of capsomer stoichiometry, since the major capsid protein accounts for a large and well-defined fraction of the molecular contents of the nucleocapsid.

MATERIALS AND METHODS

Virus growth and nucleocapsid purification. All experiments were carried out with the Kentucky A strain of EHV-1 (obtained from George Allen, University of Kentucky) which was grown on monolayer cultures of L-929 cells. The cells were propagated in Dulbecco modified minimal essential medium containing 8% newborn calf serum, 10% tryptose phosphate broth, and antibiotics. Nucleocapsids were prepared from the nuclei of infected cells essentially by the method of Perdue et al. (20). Confluent cell monolayers in 150-cm² tissue culture flasks were infected with 0.25 ml of

* Corresponding author.

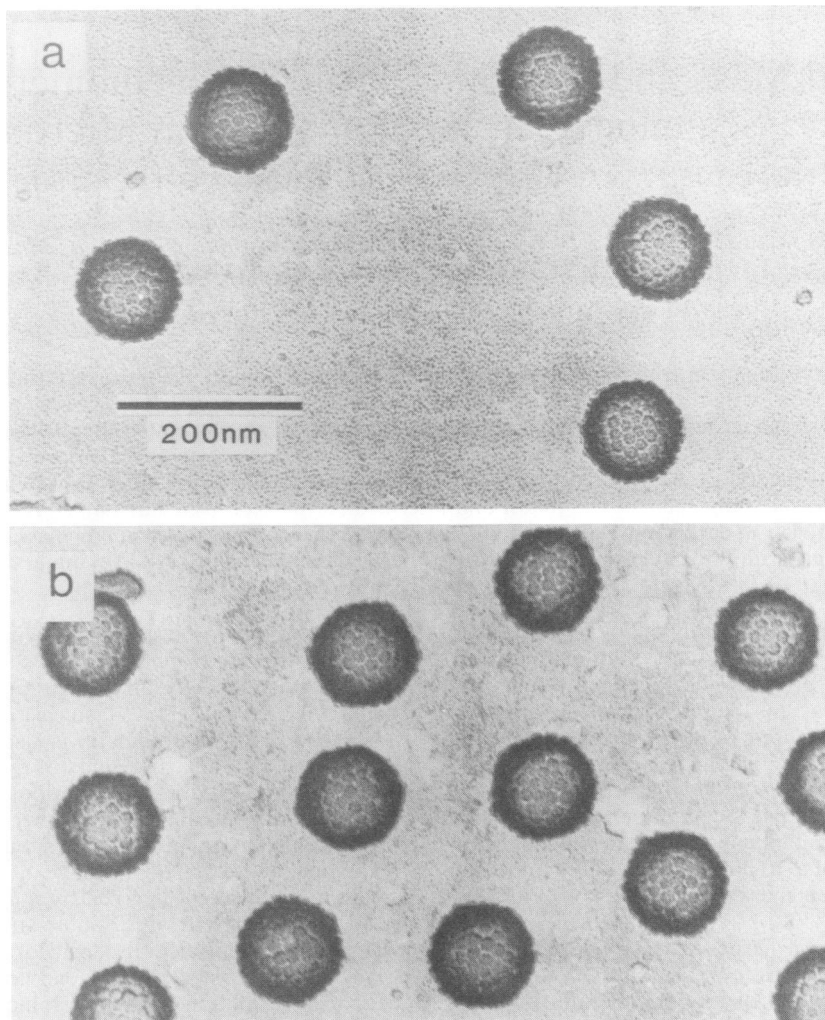


FIG. 1. Electron micrographs of EHV-1 light (a) and intermediate (b) nucleocapsids. Purified nucleocapsids were prepared for electron microscopy by critical point drying and rotary shadowing with Pt:C as previously described (16). They were photographed at a magnification of $\times 33,000$ in a JEOL 100cx electron microscope.

virus stock (in Dulbecco modified minimal essential medium containing 8% serum) at a multiplicity of infection of 1 to 4 PFU per cell. The virus was first allowed to attach for 1 h at 37°C; infection was then continued for 18 h at 37°C in 10 ml of cell growth medium (containing 2% serum rather than 8% serum). All subsequent operations were performed at 4°C. These included lysis of cell nuclei by sonication and separation of light and intermediate nucleocapsids by centrifugation on density gradients of Renografin-76 (20). After centrifugation, bands of light and intermediate nucleocapsids were removed separately from the gradient with a Pasteur pipette, diluted in TE buffer (10 mM Tris-hydrochloride, pH 7.4, 1 mM EDTA) and pelleted by centrifugation for 1 h at 24,000 rpm in an SW-28 rotor. Typical preparations beginning with 20 to 30 flasks of infected cells yielded 1 to 5 mg of light and intermediate nucleocapsids each. The yield of intermediate nucleocapsids was always greater than that of light nucleocapsids.

STEM. All STEM was carried out with the National Institutes of Health Biotechnology Resource STEM at Brookhaven National Laboratory (35, 37). Nucleocapsids were prepared for dark-field STEM microscopy by freeze-

drying them essentially by the methods of Mosesson et al. (14) and Steven et al. (28). Briefly, suspensions of nucleocapsids at approximately 0.5 mg/ml in TE were adsorbed for 5 min (by the wet film protocol [36]) to carbon-coated electron microscope grids to which tobacco mosaic virions had previously been attached. The latter were included to serve as internal mass standards. The film was then washed (eight times for 30 s each) on drops of 20 mM ammonium acetate, pH 7.0, blotted to leave only a thin layer of buffer covering the specimen, and immediately immersed in liquid N₂ slush. Freeze-drying was carried out for 6 to 8 h at a constant sublimation rate (35). Dried specimens were then transferred to the STEM and maintained at -160°C during observation. Dark-field micrographs were recorded by using the signal from the large-angle annular dark-field detector, which registers approximately 40% of the elastically scattered electrons (35). Magnifications were such that each digital scan of 512 by 512 pixels covered an area of $0.25\ \mu\text{m}^2$ (i.e., a 1-nm step per pixel).

Mass measurement by computer image processing. Digital STEM micrographs were analyzed with a VAX 11/780 computer interfaced to a Gould-DeAnza IP8500 image pro-

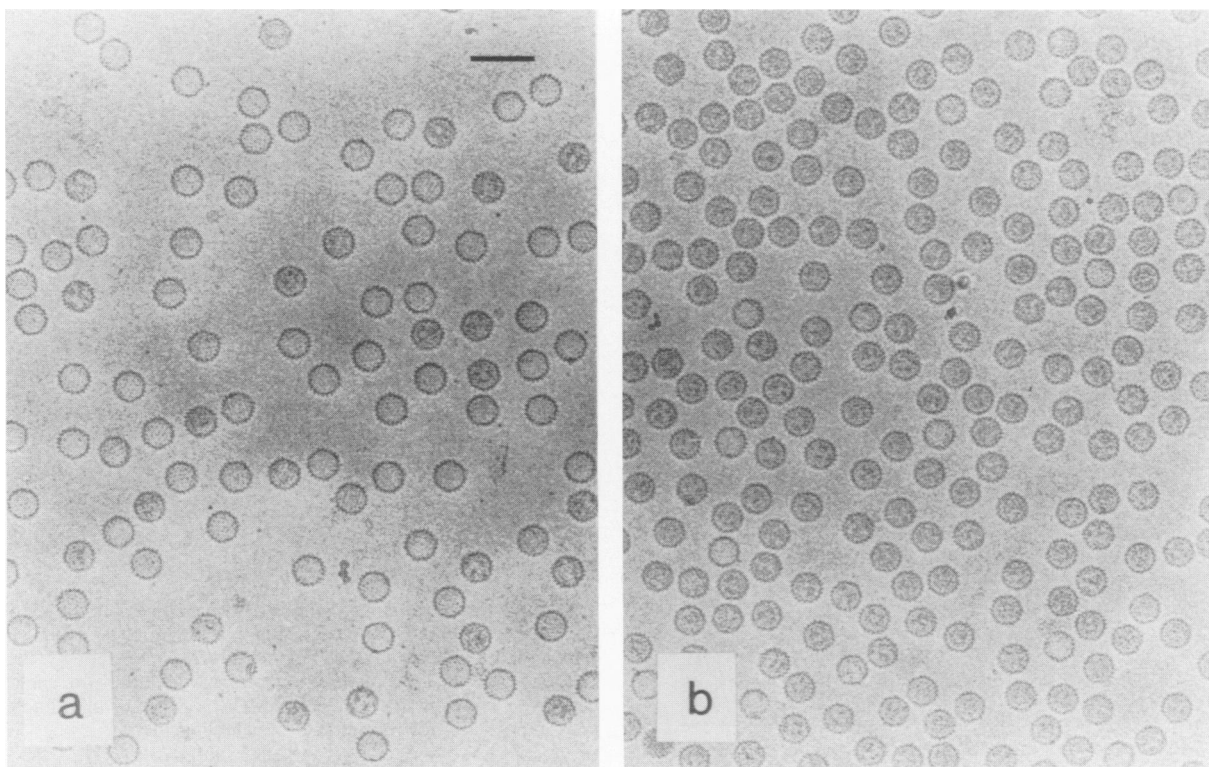


FIG. 2. Cryoelectron microscopy of EHV-1 light (a) and intermediate (b) nucleocapsids. Specimens were preserved in the frozen, hydrated state and imaged by phase-contrast transmission electron microscopy (2). We infer that the particles with additional density, apparently located inside the capsid, correspond to the true intermediate nucleocapsids. Such images, therefore, may be used to estimate the levels of cross-contamination in the respective factions. Bar, 200 nm.

cessor and a Matrix 4007 camera station. Basic image manipulation and processing operations were performed by using the PIC system (32). Mass measurements were performed basically as previously described (28, 30, 31). Micrographs were displayed on a television monitor, and particles were enclosed within contours that were traced manually on an overlay plane of the television monitor using a mouse. In each case, the contour was chosen to ensure that the entire particle, but as little surrounding background area as possible, was included. Masses were determined by integrating the densities enclosed within each contour with background subtraction (i.e., the scattering contribution from the underlying carbon film) effected on a pixel-by-pixel basis, essentially by the method of Hainfeld et al. (6). Measurements were made on all nucleocapsids that were not visibly damaged or aggregated. Each mass integral was calibrated relative to corresponding integrals for tobacco mosaic virions (131.4 kDa/nm) present in the same micrograph. Histograms were drawn, and statistical analysis of the data was carried out by using the MLAB program (10) running on a DEC-10 computer.

Other methods. Negative staining was carried out with 1% aqueous uranyl acetate as described by Thomas et al. (31). Rotary shadowing was performed with critical-point-dried specimens as described by Newcomb and Brown (16). The methods described by Booy et al. (2) were used for preparation of frozen, hydrated specimens and for their observation in the electron microscope at low temperature and low electron dose. Sodium dodecyl sulfate (SDS)-polyacrylamide gel electrophoresis and gel staining with Coomassie blue were carried out as previously described (16). The

amount of protein in individual stained bands was determined quantitatively by scanning gels in an LKB Ultrosan XL laser densitometer; the LKB 2400 Gelscan program (version 1.2) was used to integrate the data. Background staining was determined from the local areas just above and just below each peak. The protein numbering system and molecular weights were obtained from O'Callaghan and Randall (17). Total protein was measured by the Lowry (11) method. The procedures described by Maniatis et al. (12) were used for phenol extraction of DNA from nucleocapsids and for quantitative determination of DNA by fluorescence after ethidium bromide dye binding. DNA loss during phenol extraction and purification was corrected on the basis of results of control determinations in which known amounts of bacteriophage lambda DNA were subjected to the same procedures.

RESULTS

Light and intermediate nucleocapsids were purified from the nuclei of infected cells, and their respective masses were determined by STEM analysis. In complementary experiments, their protein compositions were evaluated by quantitative SDS-polyacrylamide gel electrophoresis and their DNA contents were measured quantitatively. Before analysis, nucleocapsid preparations were screened by conventional transmission electron microscopy of specimens that had been negatively stained (data not shown), shadowed after critical-point drying (Fig. 1), or preserved in the frozen, hydrated state (Fig. 2). Shadowed preparations demonstrated that nucleocapsids were morphologically intact and

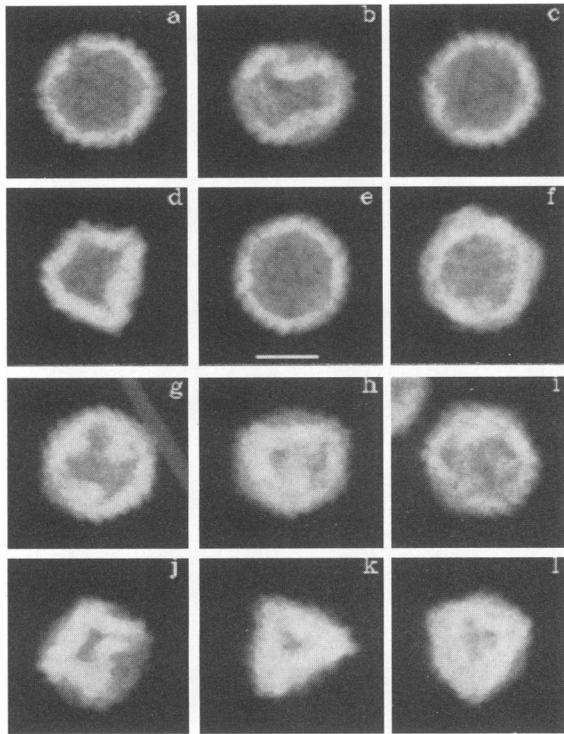


FIG. 3. STEM micrographs of EHV-1 nucleocapsids. Panels a through f are representative of the light nucleocapsid images employed for mass determinations; panels g through l show intermediate nucleocapsids. Nucleocapsids were prepared for analysis by freeze-drying without staining or shadowing, and they were imaged in the dark-field mode of the Brookhaven STEM (37). Micrographs were recorded in digital form, and the data, as shown here, have been normalized so that equal amounts of projected density are conveyed by the same grey tones in each panel. Bar, 50 nm.

substantially free from contaminating cellular material. In frozen, hydrated specimens it was possible to distinguish light from intermediate nucleocapsids and thereby estimate the level of cross-contamination in each preparation. From this analysis we conclude that 16% ($n = 1,000$) of nominally light nucleocapsids were, in fact, intermediate nucleocapsids, while preparations of intermediate nucleocapsids contained only about 3% light nucleocapsids ($n = 1,000$).

Figure 3 shows representative dark-field STEM images of the two kinds of nucleocapsids. From these micrographs, mass determinations were performed by appropriate two-dimensional integrations. Some particles were essentially undistorted after freeze-drying (e.g., Fig. 3a, c, e, and i), whereas others had undergone various degrees of flattening. Light and intermediate nucleocapsids did not differ systematically, however, in either the prevalence or degree of distortion. Moreover, there were no indications that flattening was accompanied by loss of protein; such loss would have resulted in the presence of debris in the vicinity of distorted particles and/or in such particles tending to have lower masses than unflattened ones. We observed no evidence for either effect. The mass data presented in Fig. 4 conform to unimodal distributions in both cases. The average mass (\pm standard deviation) obtained for light nucleocapsids was 196.7 ± 9.2 MDa ($n = 60$), whereas intermediates were significantly more massive, at 229.0 ± 9.5 MDa ($n = 44$).

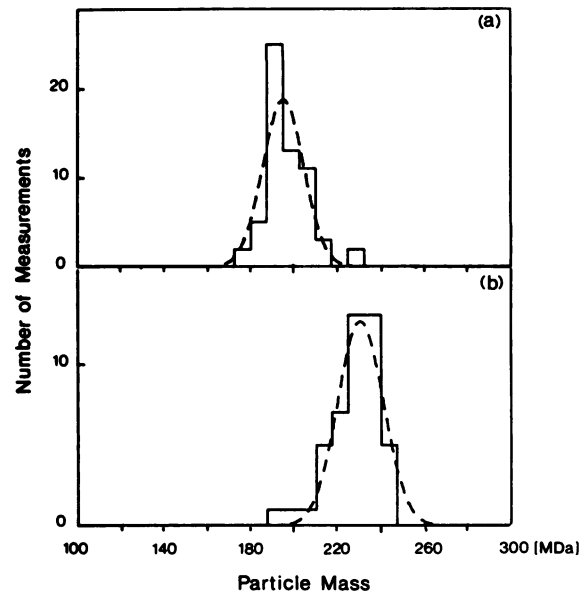


FIG. 4. Histograms showing STEM mass measurements of individual EHV-1 light (a) and intermediate (b) nucleocapsids. ---, Single-component Gaussian curves fitted to the data by the least squares method. The mean and standard deviation for each curve are given in Results. Bin size, 7.5 MDa; $n = 60$ for light nucleocapsids and $n = 44$ for intermediate nucleocapsids.

The DNA content of light and intermediate nucleocapsids was determined by quantitating ethidium bromide binding after phenol extraction. The results (Table 1) showed that both nucleocapsid types contained only vestigial amounts of DNA, equivalent to not more than 0.20% (wt/wt) or 0.4 MDa per capsid.

Protein compositions were determined by SDS-polyacrylamide gel analysis after staining with Coomassie blue. One of the gels analyzed is shown in Fig. 5, and the results are summarized in Table 2. As expected, p9 was the most abundant protein present, accounting for an estimated 66% of the total protein for light nucleocapsids and ~59% for intermediate nucleocapsids. Proteins 19 and 23 each accounted for 10 to 12% of the dye-binding material in both cases. The major difference between the two kinds of particles involved p22, which accounted for ~12% of intermediate nucleocapsid protein but was only present in trace amounts (1 to 2%) in light nucleocapsids. Overall, these data are in reasonably good agreement with the earlier determination of nucleocapsid protein composition by Perdue et al. (19).

TABLE 1. DNA contents of light and intermediate EHV-1 nucleocapsids^a

Nucleocapsid type	DNA ($\mu\text{g}/\text{mg}$ of protein) (avg \pm SD)	% DNA (wt/wt) ^b	% DNA (wt/wt) expected for full capsid ^c
Light	1.62 ± 0.74	0.16	31.8
Intermediate	0.64 ± 0.07	0.06	28.7

^a DNA was extracted and determined quantitatively from 20- μg samples of light or intermediate nucleocapsids as described in Materials and Methods. Results shown are from three independent determinations.

^b These calculations were made assuming nucleocapsids contain only DNA and protein.

^c The molecular weight of EHV-1 DNA was assumed to be 92 MDa (9).

TABLE 2. Protein composition of light and intermediate EHV-1 nucleocapsids

Protein	M_r (kDa)	% of total in light nucleocapsids ^a	Copy number in light nucleocapsids ^b	% of total in intermediate nucleocapsids	Copy number in intermediate nucleocapsids
9	148	69.3, 63.4 (69.4)	882 ± 57	58.7, 59.3 (62.0)	913 ± 38
19	59	9.2, 12.5 (10.4)	362 ± 58	10.2, 9.8 (11.5)	388 ± 18
22	46	1.0, 2.5 (ND ^c)	75 ± 32	9.0, 15.2 (9.0)	602 ± 156
23	36	13.5, 11.1 (13.8)	672 ± 73	12.0, 8.6 (11.2)	655 ± 111
24	29	0.6, ND (ND)	20 ± 20	1.5, 0.6 (<1)	83 ± 36
26	12	5.8, 10.5 (5.1)	1336 ± 390	7.8, 6.4 (5.4)	1355 ± 145

^a Percentages given are results of two independent experiments based on quantitation of Coomassie blue-stained gels. Numbers in parentheses are the results of Purdue et al. (19), which were obtained with proteins metabolically labeled with ¹⁴C-amino acids.

^b Copy numbers (N) were calculated from the measured nucleocapsid masses (M), the fractions (f) of total protein, and molecular weights (m) according to $N = (M \cdot f)/m$. Protein migrating at the dye front was assumed to be VP26, which was found by electrophoresis on 15% polyacrylamide gels to have an M_r of 12 kDa. The quoted margins of error were calculated from $(\delta N/N)^2 = (\delta M/M)^2 + (\delta f/f)^2$, where $\delta M/M$ and $\delta f/f$ were taken as the ratios of the standard deviation to the mean for the respective variables.

^c ND, Not detected.

DISCUSSION

The data obtained here (STEM measurements of the total particle mass and biochemical determinations of the relative amounts of the various nucleocapsid proteins) allow one to calculate the average copy number of each protein per particle (Table 2). The data may also be compared with particle masses predicted from the (known) numbers of hexavalent and pentavalent capsomers and the small number of viable alternatives for their stoichiometries. The only two possibilities compatible with the observed symmetry of the hexavalent capsomers are that they should be hexamers or trimers of p9 (see Introduction). An additional but lesser source of variation is whether or not the pentavalent cap-

somers are also composed of p9. Calibrating the amounts of the other proteins relative to the amount of p9 specified in each model, we obtained the predicted masses listed in Table 3. When these predictions are compared with experimental results, it is evident that only p9 hexamer models are compatible with the data. A trimer model would require that the STEM mass measurements incur a systematic overestimate of more than 70%. In the many previous applications of this technique, systematic errors have generally been much less than 10%, and in no case have they even come close to 70% (35, 37). Accordingly, we may conclude that the hexavalent capsomers of EHV-1 are based on hexamers of p9. Since all herpesviruses have similar capsid structures, it is highly likely that these results apply to them as well.

On the other hand, the STEM results do not allow one to distinguish between capsid models in which p9 constitutes (i) the hexavalent capsomers alone or (ii) both hexavalent and pentavalent capsomers. Both models predict total particle masses that lie within the experimental margin of error (cf. Table 2 and 3). Furthermore, the molecular weights used for the nucleocapsid proteins in these calculations were estimated from SDS-polyacrylamide gel electrophoresis and may easily be subject to errors on the order of 10 to 15% (2). Concerning this point, however, it is reassuring to note that where such a comparison is possible, there is generally good agreement between the molecular weights of herpesvirus nucleocapsid proteins determined from gels and those calculated from amino acid sequences deduced from cloned nucleotide sequences. In particular, the major capsid protein of herpes simplex virus type 1 has a sequence-derived molecular weight of 149,075 (13), compared with gel-based estimates of 150,000 to 155,000 (3, 26). Thus, although

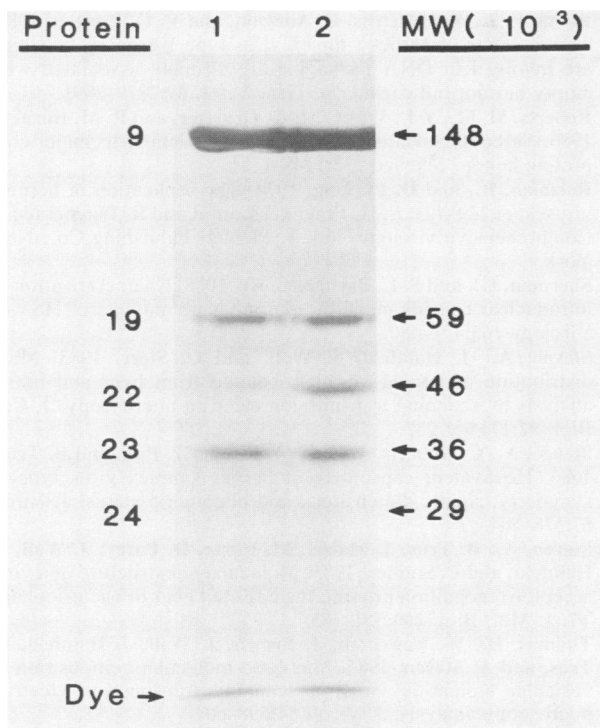


FIG. 5. SDS-polyacrylamide gel analysis of proteins from light (lane 1) and intermediate (lane 2) EHV-1 nucleocapsids. Gels were run and stained with Coomassie blue as previously described (16). Individual proteins are identified by number on the left and by molecular weight on the right.

TABLE 3. Dependence of nucleocapsid mass on capsomer protein stoichiometry

No. of copies of protein 9 per:		Predicted nucleocapsid mass (MDa) ^a	
Hexavalent capsomer	Pentavalent capsomer	Light	Intermediate
6	5	214.0	240.8
6	0	200.6	225.8
3	5	113.7	127.9
3	0	100.3	112.9

^a Masses were calculated from the M_r of protein 9, its copy number per nucleocapsid ($150 \cdot N_6 + 12 \cdot N_5$, where there are N_6 copies of protein 9 per hexavalent capsomer, etc.), and its proportional content in light (66.4%) and intermediate (59.0%) nucleocapsids (Table 2).

molecular weight errors on this scale would not effect the conclusion that the hexavalent capsomers are hexamers of p9, it is not possible to determine the pentavalent capsomers' composition on the basis of the present data.

Concerning the molecular compositions of intermediate and light nucleocapsids, the essential difference between them lies in their respective contents of p22 (Table 2). This amount of additional protein is sufficient to account for the observed difference between their respective masses. In fact, the observed level of cross-contamination of intermediates in the light nucleocapsids would be sufficient to account for the small amount of p22 associated with this fraction. It is also possible that light nucleocapsids may contain p24 in reduced amounts, although this protein is an extremely minor component and the associated margin of error is high. Thus, recalling that no significant amount of DNA was found associated with either type of particle isolated from our gradient fractions, we find that the presence of p22 in intermediate EHV-1 nucleocapsids is the only difference between them that correlates with the inferred maturability of intermediate nucleocapsids and the contrasting nonmaturability of light nucleocapsids (21).

ACKNOWLEDGMENTS

We thank J. Wall and J. Hainfeld (Brookhaven National Laboratory) for provision of data from their STEM facility, G. Shue for preparation of specimens for STEM microscopy, Elliot Mendelson for help with DNA analyses, B. L. Trus (CSL-DCRT, National Institutes of Health) for making available computing facilities for mass analyses, and J. Hay (USUHS) for useful information.

This work was supported in part by Public Health Service grant GM34036 from the National Institutes of Health.

LITERATURE CITED

- Almeida, J., D. Lang, and P. Talbot. 1978. Herpesvirus morphology: visualization of a structural subunit. *Intervirology* **10**:318-320.
- Booy, F. P., W. W. Newcomb, J. C. Brown, and A. C. Steven. 1988. Herpesvirus nucleocapsids imaged in the frozen-hydrated state, p. 164-165. *Proceedings of the 46th Annual Meeting of the Electron Microscopy Society of America*. San Francisco Press, Inc., San Francisco.
- Dargan, D. 1986. The structure and assembly of herpesviruses, p. 359-437. *In* J. Harris and R. Horne (ed.), *Electron microscopy of proteins*, vol. 5. Academic Press, Inc. (London), Ltd., London.
- Furlong, D. 1978. Direct evidence for 6-fold symmetry of the herpesvirus hexon capsomere. *Proc. Natl. Acad. Sci. USA* **75**:2764-2766.
- Gibson, W., and B. Roizman. 1972. Proteins specified by herpes simplex virus. *J. Virol.* **10**:1044-1052.
- Hainfeld, J., J. Wall, and E. Desmond. 1982. A small computer system for micrograph analysis. *Ultramicroscopy* **8**:263-270.
- Hay, J., C. Roberts, W. Ruyechan, and A. Steven. 1987. Herpesviridae, p. 391-405. *In* M. Nermut and A. Steven (ed.), *Animal virus structure*. Elsevier Biomedical Press, Amsterdam.
- Heine, J., R. Honess, E. Cassai, and B. Roizman. 1974. Proteins specified by herpes simplex virus. XII. The virion polypeptides of type 1 strains. *J. Virol.* **14**:640-651.
- Henry, B., R. Robinson, S. Dauenhauer, S. Atherton, G. Hayward, and D. O'Callaghan. 1981. Structure of the genome of equine herpesvirus type 1. *Virology* **115**:97-114.
- Knott, G. 1979. MLAB—a mathematical modeling tool. *Comput. Programs Biomed.* **10**:271-280.
- Lowry, O. H., N. J. Rosebrough, A. L. Farr, and R. J. Randall. 1951. Protein measurement with the Folin phenol reagent. *J. Biol. Chem.* **193**:265-275.
- Maniatis, T., E. F. Fritsch, and J. Sambrook. 1980. *Molecular cloning: a laboratory manual*. Cold Spring Harbor Laboratory, Cold Spring Harbor, N.Y.
- McGeoch, D. J., M. A. Dalrymple, A. J. Davidson, A. Dolan, M. D. Frame, D. McNab, L. J. Perry, J. A. Scott, and P. Taylor. 1988. The complete DNA sequence of the long unique region in the genome of herpes simplex virus type 1. *J. Gen. Virol.* **69**:1531-1574.
- Mosesson, M., J. Hainfeld, R. Haschemeyer, and J. Wall. 1981. Identification and mass analysis of human fibrinogen molecules and their domains by scanning transmission electron microscopy. *J. Mol. Biol.* **153**:695-718.
- Nermut, M. V., and W. J. Perkins. 1979. Consideration of the three-dimensional structure of the adenovirus hexon from electron microscopy and computer modeling. *Micron* **10**:247-266.
- Newcomb, W., and J. Brown. 1988. Use of Ar⁺ plasma etching to localize structural proteins in viruses: studies with adenovirus 2. *Anal. Biochem.* **169**:279-286.
- O'Callaghan, D., and C. Randall. 1976. Molecular anatomy of herpesviruses: recent studies. *Prog. Med. Virol.* **22**:152-210.
- Palmer, E., M. Martin, and G. Gary. 1975. The ultrastructure of disrupted herpesvirus nucleocapsids. *Virology* **65**:260-265.
- Perdue, M., J. Cohen, M. Kemp, C. Randall, and D. O'Callaghan. 1975. Characterization of three species of nucleocapsids of equine herpes virus type 1. *Virology* **64**:187-205.
- Perdue, M., M. Kemp, C. Randall, and D. O'Callaghan. 1974. Studies of the molecular anatomy of the L-M cell strain of equine herpes virus type 1: proteins of the nucleocapsid and intact virion. *Virology* **59**:201-216.
- Perdue, M. L., J. C. Cohen, C. C. Randall, and D. J. O'Callaghan. 1976. Biochemical studies on the maturation of herpesvirus nucleocapsid species. *Virology* **74**:194-208.
- Philipson, L. 1983. Structure and assembly of adenoviruses. *Curr. Top. Microbiol. Immunol.* **109**:1-52.
- Preston, V. G., J. Coates, and F. Rixon. 1983. Identification and characterization of a herpes simplex virus gene product required for the encapsidation of virus DNA. *J. Virol.* **45**:1056-1064.
- Rixon, F. J., A. M. Cross, C. Addison, and V. G. Preston. 1988. The products of herpes simplex virus type 1 gene UL26 which are involved in DNA packaging are strongly associated with empty but not full capsids. *J. Gen. Virol.* **69**:2879-2891.
- Roberts, M. M., J. L. White, M. G. Gruetter, and R. M. Burnett. 1986. Three-dimensional structure of the adenovirus major coat protein hexon. *Science* **232**:1148-1151.
- Roizman, B., and D. Furlong. 1974. The replication of herpesviruses, p. 229-403. *In* H. Fraenkel-Conrat and R. Wagner (ed.), *Comprehensive virology*, vol. 3. Plenum Publishing Co., New York.
- Sherman, G., and S. L. Bachenheimer. 1988. Characterization of intranuclear capsids made by morphogenic mutants of HSV-1. *Virology* **163**:471-480.
- Steven, A., J. Hainfeld, J. Wall, and C. Steer. 1983. Mass distribution of coated vesicles isolated from liver and brain: analysis by scanning transmission electron microscopy. *J. Cell Biol.* **97**:1714-1723.
- Steven, A., C. Roberts, J. Hay, M. Bisher, T. Pun, and B. Trus. 1986. Hexavalent capsomers of herpes simplex virus type 2: symmetry, shape, dimensions, and oligomeric status. *J. Virol.* **57**:578-584.
- Steven, A., B. Trus, J. Maizel, M. Unser, D. Parry, J. Wall, J. Hainfeld, and F. Studier. 1988. Molecular substructure of a viral receptor-recognition protein: the gp17 tail fiber of bacteriophage T7. *J. Mol. Biol.* **200**:351-365.
- Thomas, D., W. Newcomb, J. Brown, J. Wall, J. Hainfeld, B. Trus, and A. Steven. 1985. Mass and molecular composition of vesicular stomatitis virus: a scanning transmission electron microscopy analysis. *J. Virol.* **54**:598-607.
- Trus, B., and A. Steven. 1981. Digital image processing of electron micrographs: the PIC system. *Ultramicroscopy* **6**:383-386.
- Vernon, S., W. Lawrence, and G. Cohen. 1974. Morphological components of herpesvirus I. Intercapsomeric fibrils and the geometry of the capsid. *Intervirology* **4**:237-248.

34. **Vernon, S., M. Ponce de Leon, G. Cohen, R. Eisenberg, and B. Rubin.** 1981. Morphological components of herpesvirus III. Localization of herpes simplex virus type 1 nucleocapsid polypeptides by immune electron microscopy. *J. Gen. Virol.* **54**: 39–46.
35. **Wall, J.** 1979. Mass measurements with the electron microscope, p. 333–342. *In* J. Hren, J. Goldstein, and D. Jay (ed.), *Introduction to analytical electron microscopy*. Plenum Publishing Corp., New York.
36. **Wall, J., J. Hainfeld, and K. Cheung.** 1985. Films that wet without glow discharge, p. 716–717. *Proceedings of the 43rd Meeting of the Electron Microscopy Society of America*. San Francisco Press, Inc., San Francisco.
37. **Wall, J., and J. Hainfeld.** 1986. Mass mapping with the scanning transmission electron microscope. *Annu. Rev. Biophys. Biophys. Chem.* **15**:355–376.
38. **Wildy, P., W. Russell, and R. Horne.** 1960. The morphology of herpes virus. *Virology* **12**:204–222.